Eur Phys J C **32** (s02), 55–67 (2003)
Digital Object Identifier (DOI) 10.1140/epjcd/s2003-01-016-2

EPJ C direct
electronic only

Prospects for observing the Kaluza-Klein excitations of the W boson in the ATLAS detector at the LHC

G. Polesello and M. Prata

INFN, Sezione di Pavia, Dipartimento di Fisica Nucleare e Teorica, Universitá di Pavia, Via Bassi 6, Pavia, Italy

Received: 9 Sep 2003 / Accepted: 19 Nov 2003 /
Published Online: 17 Dec 2003 –

Abstract. Kaluza-Klein excitations of the gauge bosons are a notable feature of theories with "small" ($\sim$ 1 TeV) extra dimensions. The leptonic decays of the excitations of the W boson provide at the LHC the striking signature of events containing an isolated high P_T lepton accompanied by a high transverse momentum imbalance.
We investigate the reach for these signatures through a parametrized simulation of the ATLAS detector. With an integrated luminosity of 100 fb^{-1} a peak in the transverse invariant mass of the lepton-neutrino system will be detected if the compactification scale (M_c) is below 6 TeV. If no signal is observed, with an integrated luminosity of 100 fb^{-1} a limit of $M_c > 11.7$ TeV can be obtained from the study of the lepton-neutrino transverse mass distribution below the peak. If a peak is detected, a measurement of the couplings of the boson to leptons and quarks can be performed for M_c up to $\sim$ 5 TeV.

PACS. 11.10Kk – 11.25Mj – 13.85-t

In recent years models incorporating additional spatial dimensions have enjoyed much theoretical interest, as a promising path toward accounting for the large gap between the scale characteristic of the gravitational interactions and the TeV scale.

The ADD model [1], the first and best studied among these models, postulates n "large" extra dimensions, in which gravity propagates. These are compactified at a scale $1/R_c$. In order to make the fundamental scale of the gravitational interactions in $4+n$ dimension as low as a few TeV, the compactification scale must be in the 10^{-2} eV to a few MeV range. Any field which propagates in the "bulk" has Kaluza-Klein (KK) excitations with mass of the order of the compactification scale. Such states are forbidden for the Standard Model (SM) gauge fields by the results from high energy experiments which put a lower limit of around 1 TeV on them. Therefore in a model in which the extra dimensions are characterized by compactification radii $R_c \gg 1$ TeV^{-1}, only gravity propagates in the bulk and the SM gauge fields are confined to a 3-brane. This is a characteristic feature of a class of models in which all of the extra dimensions have the same compactification radius. Such a scenario could be probed by searching for the graviton KK excitations at the future high energy accelerators, and the corresponding signatures have been the subject of a large number of phenomenological studies [2].

It is however possible to formulate models with asymmetrical extra dimensions, in which some of them have the "large" size, required to solve the hierarchy problem, but some "small" additional extra dimensions exist, with $R_c \sim 1$ TeV^{-1}, in which the gauge and matter fields can propagate. Several variations on this basic pattern, depending on which fields are allowed in the bulk, can be found in the literature [2]. We restrict our phenomenological study to a model where only the fermions are confined on the 3-brane [3], [4], whereas all the SM gauge and Higgs fields propagate in the "small" extra dimension.

The boson excitations couple to the fermions on the 3-brane with couplings equal to the SM ones multiplied by a factor which depends on the number of extra dimensions in which the gauge fields propagate, and on the details of the compactification. For definiteness, we assume only one additional "small" extra dimension, compactified on S^1/Z^1, where all the fermions are at the same orbifold point ($D = 0$). This model is completely specified by a single parameter $M_c = 1/R_c$, the compactification scale, and the masses of the gauge boson KK modes are given by the relation:

$$M_n^2 = (nM_c)^2 + M_0^2 \tag{1}$$

where M_0 is the mass of the zero mode excitation, corresponding to the Standard Model gauge boson, and n is the KK mode. The couplings are the same as the corresponding SM couplings scaled by a factor $\sqrt{2}$. In the case of more than one additional dimension, the mass and coupling pattern will be much more complex, yielding a markedly different phenomenology.

The constraints on the compactification scale from precision electroweak measurements have been evaluated in a number of papers [5], [6], and [7]. These limits are essen-

tially based on predicting deviations from the electroweak expectations due to new contact interactions calculated by integrating over the exchange of the full tower of KK fields. The sum over the KK states is divergent for more than one extra dimension, and a regularization procedure must be adopted, which introduces an uncertainty on the model limits. In the case of one "small" extra dimension, the sum is finite, and yields an approximate 4 TeV lower limit on the compactification scale for the reference model considered in this analysis.

The main experimental signature at LHC will be the direct observation of KK excitations of the SM gauge bosons, i.e. the gluon, the photon, the W and the Z. Since we are considering M_c in the few TeV range, from (1), the excitations of all the gauge bosons for a given n are essentially degenerate in mass. The gluon excitations are the most abundantly produced, but they decay into quark pairs, with a width proportional to α_s, and therefore their decay will be hardly detected over the overwhelming jet-jet continuum QCD background. Much better hope for discovery is provided by the leptonic decays of the γ, Z and W excitations. The neutral decays into two charged leptons have been the subject of a few phenomenological studies, also because the neutral KK bosons can be produced in e^+e^- collisions, and their properties could be studied with great precision at the future e^+e^- colliders, even at center-of-mass energies well below the scale M_c. A detailed experimental study of the $\gamma^{(1)}/Z^{(1)}$ detectability at LHC in the leptonic decay channel was also recently performed [8], yielding a sensitivity up to $M_c \sim$10 TeV for an integrated luminosity of 100 fb^{-1}. Some attempts to discriminate the Kaluza-Klein resonance from the Z' predicted in models with extended gauge group have also been performed [9]. A specific feature of our model is the presence of a $W^{(1)}$ boson with the same mass as the Z resonance. The observation of a charged partner would restrict the class of models compatible with the observed phenomenology. We are not aware of any detailed study, even at the phenomenological level, of the experimental signatures for the KK $W^{(1)}$ production. It is therefore worth assessing the ATLAS potential for the discovery of the leptonic decays of the KK excitations of the W boson.

In the following we will first describe in detail the signal simulation, and the adopted formalism. We will then address in a model independent way the $W^{(1)}$ detectability through the observable deviations from the SM expectations. Further, we will study in detail the experimental sensitivity on our reference model with a likelihood method. An attempt at measuring the $W^{(1)}$ coupling to fermions and a study of the signal, aimed at discriminating among the various possible models, will conclude the analysis.

1 Signal simulation

As discussed in the previous section, we address an experimental signature consisting in the production of a tower of resonances $W^{(n)}$ of the SM W bosons, with masses M_n given by (1).

These resonances, as the SM W, only couple to the left-handed fermion doublets, and the interaction is uniquely defined by two universal couplings $g^e(n)$ and $g^q(n)$, to the lepton and quark families, respectively. The values of the couplings result from the normalisation of the gauge field kinetic energies, and are dependent from n for a number TeV^{-1}-size extra dimensions larger than one. In this case they will also be dependent on the compactification scheme, as discussed in [6].

The parton level cross section for an electron-neutrino pair in hadronic interactions can be written as:

$$\frac{\mathrm{d}\hat{\sigma}}{\mathrm{d}\cos\theta}[u_i\bar{d}_j \to e^+\nu] = \frac{\pi\alpha^2\hat{s}}{48\sin^2\theta_W}|V_{ij}|^2\Big\{|\mathcal{M}|^2(1+\cos\theta)^2\Big\} \quad (2)$$

where

$$\mathcal{M} = \frac{g^q g^e}{\hat{s}-M_W^2+i\Gamma_W M_W} + \sum_{n=1}^{\infty}\frac{g^q(n)g^e(n)}{\hat{s}-M_n^2+i\Gamma_n M_n} \quad (3)$$

The first term in the sum is the SM W production, where we have put in evidence the SM couplings g^e and g^q, which have the values $g^e = g^q = 1$.

As a first step in simplifying the above expression, we assume that all the fermions are localized on the same brane, which implies $g^e(n) = g^q(n) \equiv g(n)$.

Given the existing limits on M_c, $M_c \gg M_W$, one can substitute $M_n = nM_c$ in (3). The decay channel $W^{(n)} \to WZ$ is forbidden by KK number conservation [10], leaving only the $W^{(n)}$ decay to fermions. Therefore, the approximate width Γ_n, neglecting QCD corrections and the kinematic factor from the top mass, can be easily estimated as:

$$\Gamma_n \simeq \frac{\Gamma_W}{M_W}\left(\frac{g^e(n)^2}{3}+g^q(n)^2\right)M_n \simeq g(n)^2\frac{\Gamma_W}{M_W}(1+\frac{1}{3})M_n \simeq g(n)^2 KnM_c \quad (4)$$

with the constant $K \simeq 0.034$. At LHC, the experiments can probe a partonic level $\hat{s}$ up to $\sim 4-5$ GeV, and the full Breit-Wigner shape is only relevant for the first N_r KK resonances. Using the above approximations, Equation (3) can be rewritten as:

$$\mathcal{M} \simeq \frac{g^q g^e}{\hat{s}-M_W^2+i\Gamma_W M_W} + \sum_{n=1}^{N_r}\frac{g^q(n)g^e(n)}{\hat{s}-M_n^2+i\Gamma_n M_n} - \frac{1}{M_c^2}\sum_{n=N_r+1}^{\infty}\frac{g^q(n)g^e(n)}{[1-ig(n)^2K]n^2} \quad (5)$$

The last term in (5) only converges for a model with only one TeV^{-1}-size extra dimension, which has $g^e(n) = g^q(n) = \sqrt{2}$ for all the KK resonances. In this case the factors involving $g^q(n)$ and $g^e(n)$ can be taken out of the sum, which reduces to:

$$\sum_{n=N_r+1}^{\infty}\frac{1}{n^2} = \pi^2/6 - \sum_{n=1}^{N_r}\frac{1}{n^2}$$

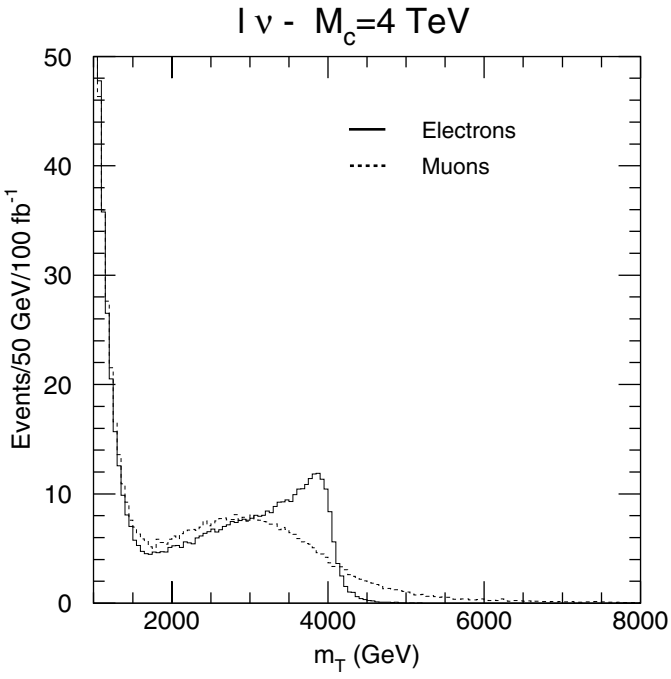

Fig. 1. Lepton-neutrino invariant transverse mass for electrons (*full line*) and muons (*dashed line*). The distribution assumes 4 TeV for the mass of the lowest lying KK excitation. The histograms are normalized to 100 fb^{-1}

For models with more than one extra dimension the sum does not converge, and various prescriptions can be adopted in order to obtain a finite prediction, as discussed in detail in [5]. We limit ourselves to the one-dimensional case considering all the terms of (5).

We stress here that it is important to consider the full expansion and not just the first few resonances. In fact, although limiting the expression to only the first two resonances does not alter the results for the reach in the peak region, it significantly underestimates the sensitivity in the low-mass off-peak region. Since the dominant contributions to the low $\hat{s}$ off-resonance region come from the interference between SM W and the KK excitations, the total deviation from the SM predictions is approximately proportional to $\frac{1}{M_c^2}\sum_{n=1}^{\infty}\frac{1}{n^2}$ and increases by $\sim 30\%$, i.e. $\left(\frac{\pi^2/6}{1.25}-1\right)$ when the full tower of resonances is considered instead of just the first two.

We use the expression (5) with $N_r = 2$ to calculate the partonic cross section according to (2), which is then convoluted with the parton distribution functions of the proton. The process thus calculated has been externally interfaced to PYTHIA 6.152 [11] event generator. The generated events have been passed through the fast simulation of the ATLAS detector [12].

As discussed in the introduction, the lowest M_c considered in this study is 4 TeV, consistent with precision electroweak measurements. It is therefore necessary to detect and measure leptons with momenta in the range of a few TeV, where the energy resolution for electrons is dominated by a constant term due to the imperfect knowledge of the EM calorimeter performance. From comparison of data from beam tests and the results of detailed detector simulation, for energies up to a few hundred GeV, this term has been evaluated below 1%. Detailed studies need to be performed to evaluate how well these results extrapolate to the momentum range of interest for this analysis. The standard parametrization included in the ATLFAST program is used for the simulation: it yields a resolution of $\sim 0.7\%$ for the energy measurement of 2 TeV electrons. This is certainly optimistic, and full simulation studies of TeV scale electrons are needed in order to achieve a proper estimate of the resolution. However, the natural width of the bosons is of order 7% from (4), and dominates the experimental resolution. The results of this study are therefore not affected by this approximation.

For high-p_T muons, the transverse momentum measurement is achieved through the sagitta measurement in the precision drift chambers, and for a 2 TeV muon the resolution is of the order of 20%. Therefore the shape of the experimental distributions will be dominated by the natural width for electrons and by the experimental momentum resolution for muons.

This is clearly seen *e.g.* in the distribution of the transverse mass m_T of the lepton and of the neutrino, defined as:

$$m_T^{\ell\nu} = \sqrt{2p_T^{\ell}p_T^{\nu}(1-\cos\Delta\phi)} \qquad (6)$$

where $\ell = e, \mu$, and $\Delta\phi$ is the angle in the transverse plane between the momenta of the neutrino and of the charged lepton. The lepton transverse momentum is directly measured, whereas the neutrino transverse momentum p_T^{ν} is obtained from the vector sum of the lepton transverse momentum, and of the transverse momentum of the hadronic system recoiling against the $W^{(1)}$. In Fig. 1 we show the distribution invariant transverse mass spectra for a 4 TeV KK resonance ($W^{(1)} \to \ell^{\pm}\nu$) both for electrons (full line) and muons (dashed line). The muon peak is much broader, giving little contribution to the precision of the $W^{(1)}$ mass measurement, but both lepton species can be used in order to observe the existence of an excess in the peak region with respect to the Standard Model.

2 $W^{(1)} \to \ell^{\pm}\nu$ channel: Data analysis

The observation of the $W^{(1)}$ is based on the detection of an excess of events with a single high p_T lepton and E_T^{miss} over the SM background. In order to select a $W^{(1)}$ sample we require:

- an isolated charged lepton ℓ (e or μ) with $p_T > 200$ GeV in the pseudorapidity range $|\eta| < 2.5$;
- missing transverse energy $E_T^{miss} > 200$ GeV;
- transverse invariant mass $m_T^{\ell\nu} > 1000$ GeV.

The isolation criterion consists in requiring a transverse energy deposition in the calorimeters smaller than 10 GeV in a (η, ϕ) cone of radius 0.2 around the lepton direction, where η is the pseudorapidity of the lepton and ϕ the angle in the plane transverse to the beam.

Table 1. Expected number of events in the peak for an integrated luminosity of 100 fb^{-1}, for different values of the mass of the lowest lying KK excitation, and Standard Model background. The peak region is defined by requiring a minimum $\ell^{\pm}\nu$ invariant transverse mass as shown in the second column. The results for electrons and muons are given separately

M_c (GeV)	M_{cut} (GeV)	$N(e)$	$N_B(e)$	$N(\mu)$	$N_B(\mu)$
4000	3000	204	2.43	171	5.12
5000	4000	26	0.13	20	1.78
6000	4000	6.1	0.13	4.5	1.78
7000	5000	0.8	0.009	0.5	1.26
8000	6000	0.1	0.001	0.1	1.07

From the cross section formula (5), it can be seen that the deviation of the $pp \to \ell\nu + X$ cross section begins to be significant for $\hat{s}$ of the order of M_c. We therefore apply a lower cut on transverse mass to select the relevant kinematic region.

The following reducible backgrounds were considered: $t\bar{t}$, with one of the two top quarks decaying leptonically, and vector boson pair production: WW, WZ, ZZ. With the applied cuts ~ 75 events are expected for a transverse mass above 1000 GeV (Fig. 2) for each lepton flavour. This background is dominated by WW and WZ production. A moderate jet veto requiring no jet in the event with p_T in excess of 100 GeV would reduce the background to ~ 20 events. All the number of events are relative to one LHC year at high luminosity (100 fb^{-1}).

In absence of new physics, approximately 500 events from SM off-shell W production survive the cuts for each of the lepton flavours.

As is well known from the study of the W boson, the distributions of the variables p_T^{ℓ}, E_T^{miss}, and $m_T^{\ell\nu}$ show a characteristic Jacobian peak, whose edge shape can be used to measure the mass and width of the resonance. The distribution of $m_T^{\ell\nu}$, being less sensitive to the modeling of the transverse momentum of the resonance is normally used for the mass measurement.

The $m_T^{e\nu}$ spectrum for a 4 TeV $W^{(1)}$ (Fig. 2) superimposed on SM $pp \to e\nu$ production shows a suppression of the cross section for masses below the resonance. This is due to the negative interference terms between SM gauge bosons and the whole tower of KK excitations, and is sizable even for compactification masses well above the ones accessible to a direct detection of the mass peak. This shape is the consequence of the model choices requiring both the leptons and the quarks to be at the same orbifold point. Alternate model choices [13] may yield opposite signs for the lepton and quark couplings to the KK resonances, and therefore reverse the sign of the interference term.

The reach for the observation of a peak in the m_T distribution can be naively estimated from Table 1, which, both for electrons and muons, gives the number of observed (N) and background (N_B) events for different values of M_c (Fig. 3). For each value a different cut M_{cut} on $m_T^{\ell\nu}$ was chosen, with the aim of optimizing the signal

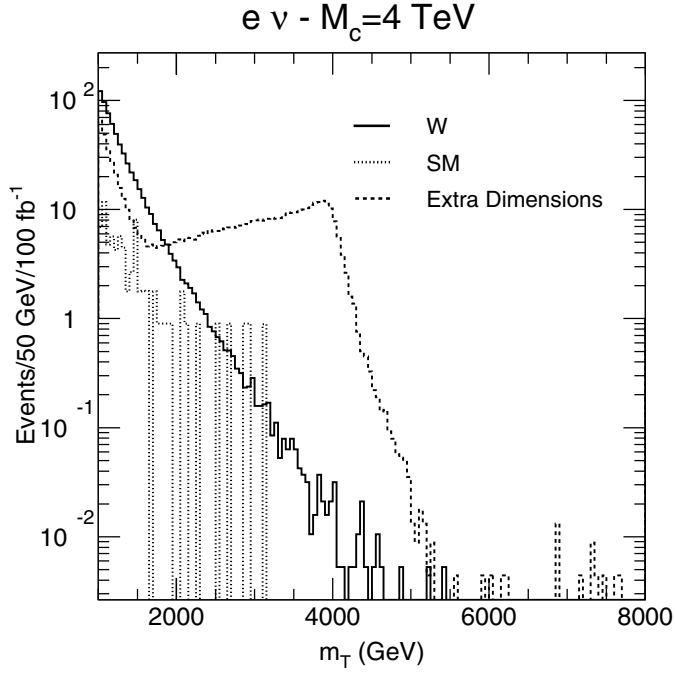

Fig. 2. Invariant transverse mass distribution of $e^{\pm}\nu$ for the Standard Model W production (*full line*), for the extra dimension model studied (*dashed line*) and for reducible SM backgrounds (*dotted line*). The mass of the lowest lying KK excitation is 4 TeV. The histograms are normalized to 100 fb^{-1}

significance. If we pose as an arbitrary requirement for the observation of the peak:

- at least 10 events summed over the two lepton flavours $[N(e) + N(\mu)]$;
- a statistical significance $\frac{(N-N_B)}{\sqrt{N_B}} \geq 5$

we obtain a reach of ~ 6.0 TeV. Even for the lowest allowed value of M_c (4 TeV), no events can be observed for the second resonance at 8 TeV, which would have been a "smoking gun" signature for this kind of model.

In order to fully evaluate the off-resonance sensitivity to interference effects, a likelihood fit to the expected spectrum can be performed and will be discussed in the next section. As a first approach, one can simply evaluate, in the interference region, the variation in number of events within a given $m_T^{\ell\nu}$ range, as a function of M_c. The $m_T^{\ell\nu}$ spectrum in the window between 1 and 2 TeV for the Standard Model and for three choices of M_c is shown in Fig. 4. The statistical significance of the cross section suppression can again be naively parametrized as $\frac{|(N-N_B)|}{\sqrt{N_B}}$ One can see that the deviation from the SM extends below the arbitrary limit of 1000 GeV on $m_T^{\ell\nu}$, and therefore one could extend the significance calculation. On the other hand, a relevant variable which should also be considered is the ratio N/N_B, since the systematic uncertainty in our knowledge of the shape of $m_T^{\ell\nu}$ sets a limit on the detectable value of this ratio. A lowering of the limit on $m_T^{\ell\nu}$ would somewhat increase the statistical significance, at the price of a significant worsening of the N/N_B, and therefore an increase of sensitivity of the result to systematic effects.

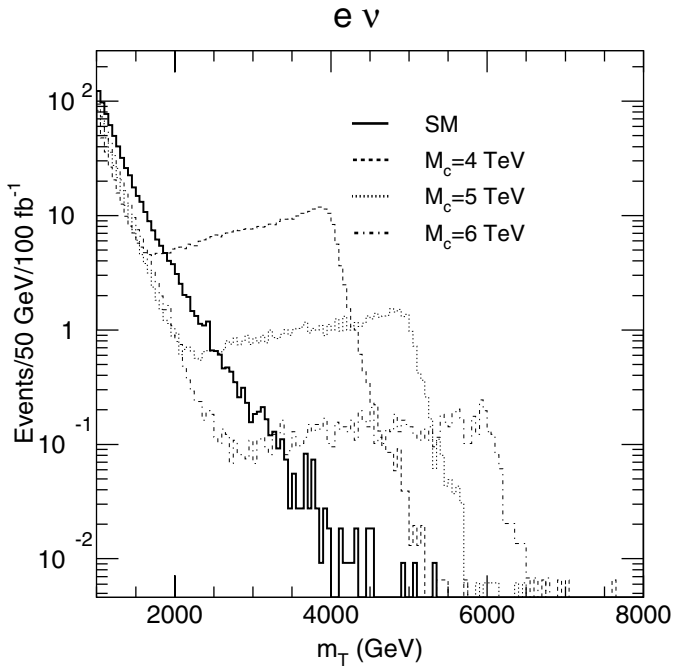

Fig. 3. Invariant transverse mass distribution of $e^{\pm}\nu$, for the extra dimension model studied, for different values of the compactification scale M_c. The histograms are normalized to 100 fb^{-1}

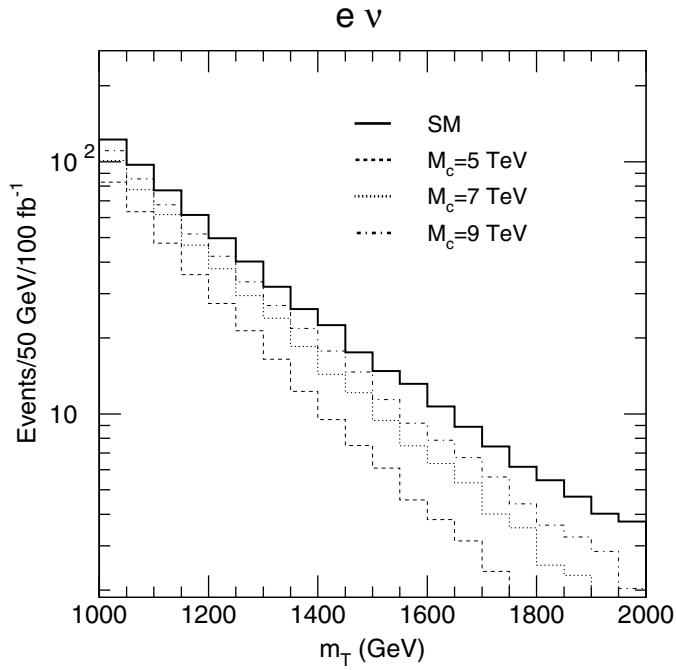

Fig. 4. Transverse-mass distribution of $e^{\pm}\nu$ in the region below 2 TeV. The Standard Model contribution is shown as a thick line. Three different values for the compactification scale M_c of the reference model are shown: 5 TeV (*dashed line*), 7 TeV (*dotted line*) and 9 TeV (*dashed-dotted line*). The histograms are normalized to 100 fb^{-1}

Table 2. Expected number of events in the interference region for an integrated luminosity of 100 fb^{-1}, for different values of the compactification scale M_c and Standard Model background. The considered mass interval is $1000 < m_T^{\ell\nu} < 2000$ GeV

M_c (GeV)	$N(e)$	$N(\mu)$
SM	692	677
4000	365	369
5000	418	412
6000	486	477
7000	534	525
8000	574	563
9000	596	583
10000	619	604
11000	628	614
12000	639	626

For this analysis a mass interval $1000 < m_T^{\ell\nu} < 2000$ GeV was chosen as a reasonable compromise, and the corresponding number of observed events for background and signal for 100 fb^{-1} are given separately for electrons and muons in Table 2. All the numbers in the table include a contribution of respectively 67 (62) events for electrons (muons) expected from reducible backgrounds. If both lepton flavours are considered, the ATLAS 5σ reach is ~ 9 TeV for an integrated luminosity of 100 fb^{-1}. The deviation from the Standard Model will be 15% for 9 TeV, defining the level of systematic control on the relevant region of the transverse mass spectrum we need to achieve in order to exploit the statistical power of the data.

3 Measurement of the compactification scale

In the previous section the experimental observability of the model under consideration has been evaluated in a model-independent way by simple event counting, providing an estimate of the M_c range within which LHC will be able to observe a peak and/or an off-peak deviation from the Standard Model in the $m_T^{\ell\nu}$ distribution.

In order to obtain a precise measurement of the model parameters and to evaluate in an optimal way the reach of the ATLAS experiment, we need to postulate a specific model, in our case a model with a single extra dimension with compactification scale M_c. Using the detailed prediction for the model, an optimal estimate of the reach can be obtained by performing a likelihood fit to the transverse mass shape expected for different values of M_c.

3.1 Likelihood fit on simulated data

We estimate M_c by performing a likelihood fit on the distribution of the transverse mass variable (Fig. 5). An important part of the information on M_c is contained in the upper edge of the distribution. Since for muons the edge is essentially washed out by the experimental resolution on the momentum measurement, as shown in Fig. 1, we only consider the $W^{(1)}$ decays into electrons. The likelihood function is calculated according to [14]:

$$-2\ln\mathcal{L} = \sum_i \left[2(N_i^{th} - N_i) + 2N_i \ln\left(\frac{N_i}{N_i^{th}}\right)\right] = \chi^2 \quad (7)$$

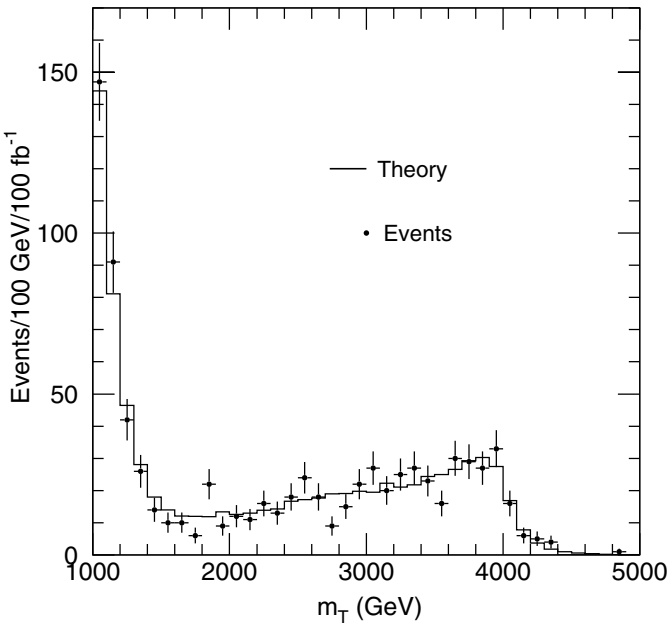

Fig. 5. $e^{\pm}\nu$ Transverse mass distribution for a simulated 100 fb^{-1} experiment for the case $M_c = 4$ TeV (*black dots*). Superimposed is the theoretical distribution (*full line*)

Table 3. Average estimated value (M_L) and r.m.s. of the compactification scale M_c for ~ 5000 Monte Carlo experiments at an integrated luminosity of 100 fb^{-1}. In the fourth and fifth columns, the mean value and the standard deviation of the Gaussian fit are given. For $M_c \geq 6$ TeV the fit was performed starting from the $1/M_c$ value corresponding to the half height of the distribution on the left side of the peak

M_c (GeV)	$\langle M_L \rangle$ (GeV)	*r.m.s.* (GeV)	M_{fit} (GeV)	σ (GeV)
4000	4001	25	4001	25
5000	5008	74	5008	73
6000	6018	145	5997	121
7000	7119	463	6984	285
8000	8116	743	7923	519

where N_i and N_i^{th} are the observed and theoretical contents of the i^{th} bin. In bins where $N_i = 0$ or $N_i^{th} = 0$, the second term is zero. Equation (7) has the advantage over a standard likelihood function to behave asymptotically like a classical χ^2.

In order to evaluate the uncertainty on the M_c measurement, for each input M_c value an ensemble of Monte Carlo experiments (100 fb^{-1} each) was generated, for each of them, the parameter $1/M_c^2$ was estimated by maximizing the likelihood function calculated with respect to a set of theoretical histograms on the $m_T^{\ell\nu}$ interval 1000-10000 GeV. These were produced by varying the value of $1/M_c^2$ in the range $\frac{1}{15000^2} \leq \frac{1}{M_c^2} \leq \frac{1}{3000^2}$ GeV^{-2} in 500 equally spaced steps. The likelihood fit is performed on the variable $1/M_c^2$ since, for $m_T^{\ell\nu} \ll M_c$, it is the natural choice for the deviation of the cross section from the Standard Model, as shown in (5). With respect to this variable, the Standard Model is the limit corresponding to $1/M_c^2 = 0$.

In Fig. 6 we show the distributions of the estimated values of $1/M_c^2$ for the ensemble of Monte Carlo experiments generated for M_c = 5, 6, 7 and 8 TeV, respectively. As expected, the distributions are Gaussian as long as events in the peak exist. Tails start to appear for $M_c = 6$ TeV for which, in average, only 4 to 6 events appear in the peak region. For $M_c \geq 7$ TeV, when less than 1 event is observed in the peak, the mass estimate entirely relies on the interference region between 1 and 2 TeV, and the distribution becomes very broad and exhibits large tails.

The average and r.m.s. of the estimated values of M_c are given in Table 3. The statistical error is below the percent level as long as events are observed in the peak region.

The likelihood formula used can be in principle employed for goodness-of-fit evaluation, but in practice the fact that the fit includes many low-population bins does not allow us to use it for this purpose. Therefore we have verified the goodness-of-fit with the Kolmogorov test, which yielded excellent agreement between the generated data sample and the theoretical invariant mass distribution for all considered values of M_c. Since the same input model was used for the generated events and for the theoretical histograms, this agreement provides a consistency check on the employed analysis procedure.

3.2 Experimental sensitivity

The experimental sensitivity is defined as *the average upper limit that would be obtained by an ensemble of experiments with the expected background and no true signal* [15].

In order to evaluate the sensitivity we generated an ensemble of $\sim$ 12000 experiments for which only SM $pp \to e^{\pm}\nu$ was present in the data. The interval for fitting was defined from $-\frac{1}{5000^2}$ to $\frac{1}{5000^2}$ GeV^{-2}, including unphysical negative values of the parameter in order to properly account for the statistical fluctuations of the SM background in all directions. The 95% CL upper limit for each Monte Carlo experiment was evaluated according to the following prescription, corresponding to a Bayesian approach with the assumption of a uniform prior probability distribution function, over the allowed physical region $1/M_c^2 > 0$:

- for each Monte Carlo experiment the likelihood function $\mathcal{L}$ was built as a function of $1/M_c^2$, where $\mathcal{L} = e^{-\chi^2/2}$ (7), and it is used here as the probability density function of $1/M_c^2$;
- the 95% CL was defined as the value of M_c such that the integral of $\mathcal{L}$ between 0 and $(1/M_c^{(95\%\ CL)})^2$ accounts for the 95% of the integral between 0 and $+\infty$:

$$M_c^{(95\%\ CL)}:$$

$$\int_0^{[1/M_c^{(95\%\ CL)}]^2} \mathcal{L}\, d\frac{1}{M_c^2} = 0.95 \int_0^{+\infty} \mathcal{L}\, d\frac{1}{M_c^2}$$

- the average value of the upper limits so obtained provides an estimate of our experimental sensitivity.

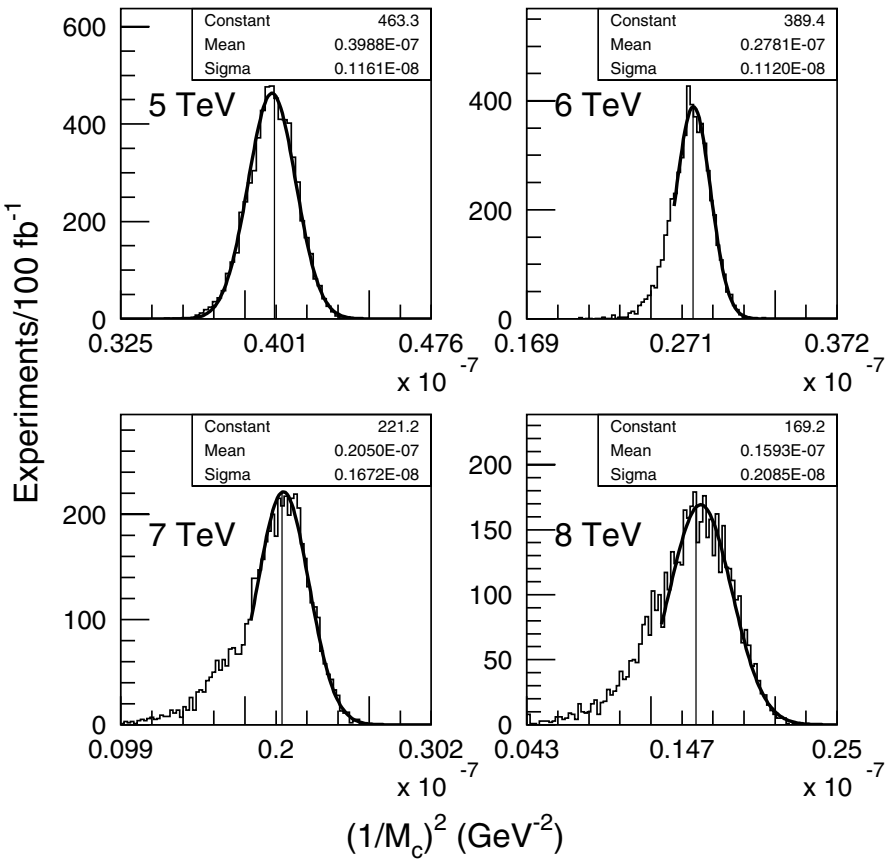

Fig. 6. $1/M_c^2$ values estimated through the maximum likelihood method for a set of ~ 5000 Monte Carlo experiments for the generated values: **a** $M_c = 5$ TeV; **b** $M_c = 6$ TeV; **c** $M_c = 7$ TeV; **d** $M_c = 8$ TeV. For $M_c \geq 6$ TeV the Gaussian fit was performed by starting from the $1/M_c^2$ value corresponding to the half height of the distribution on the left side of the peak. The integrated luminosity is 100 fb^{-1}

With this approach, for an integrated luminosity of 100 fb^{-1}, statistical sensitivity of the ATLAS experiment to the considered model is evaluated to be ~ 11.7 TeV. For a detailed estimate of the experimental sensitivity all the possible sources of systematic uncertainties must further be taken into account.

4 Systematic uncertainties

Any uncertainty in the modeling of the $W^{(1)}$ production mechanism or in the modeling of the detector response will introduce systematic errors on the estimated value of the $W^{(1)}$ mass.

An excellent evaluation of the possible sources of systematics was performed on real data by the UA2, CDF and D0 collaborations for the precision measurement of the SM W mass. This work was further expanded upon in [17] and in [18], where the results were extrapolated to the performance of the ATLAS detector. We will take these studies as a guidance, taking into account the very different energy scale with respect to the present analysis.

The basic detector-related uncertainties include the knowledge of: the lepton energy and momentum scale, the energy and momentum resolution, the detector response to the recoil fragments and the effect of the lepton identification cuts. The uncertainties related to the physics also include the knowledge of: the $W^{(1)}$ p_T spectrum and angular distribution, higher-order electroweak effects, and the parton distribution functions (PDF).

The uncertainty on the lepton energy scale is the most important of the detector-related effects. As discussed in the previous section, the statistical error on the mass measurement goes from $\sim 0.5\%$ at 4 TeV, to $\sim 2\%$ at 6 TeV, the highest value for which events are observed in the peak. Therefore an uncertainty of the lepton scale at the percent level for leptons of a few TeV is required to fully exploit the statistical power of the data. The energy scale will be fixed to better than 0.1% at 90 GeV, using the Z boson [17]. By using the production of Z bosons with high transverse momentum, it will be possible to trace the evolution of the detector linearity up to a few hundred GeV, and extrapolations based on detailed simulations of the detector will be used for higher energies. Detailed detector studies, outside the scope of this analysis, will be needed in order to evaluate if the performance goal can be achieved by ATLAS. The p_T of the neutrino is determined as the vector sum of the transverse momenta of the lepton and of the hadronic recoil energy. The hadronic component is basically composed of soft hadrons, to which, one has to add

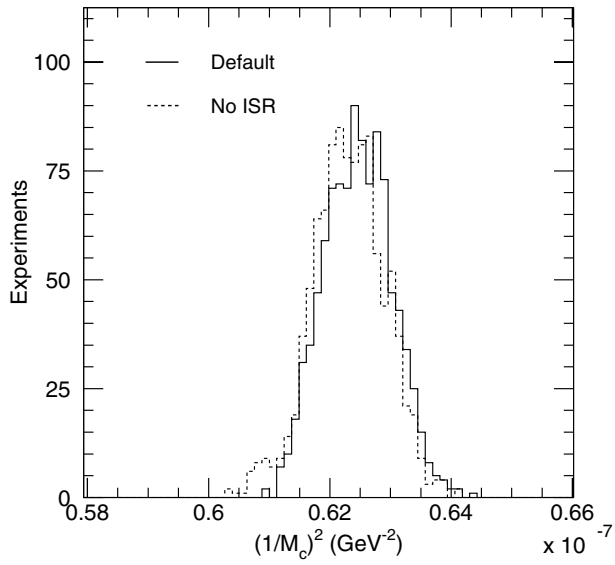

Fig. 7. Distribution of the estimated $1/M_c^2$ values for a standard data set (*full histogram*) and for the set of experiments generated with no initial state radiation (*dashed histogram*)

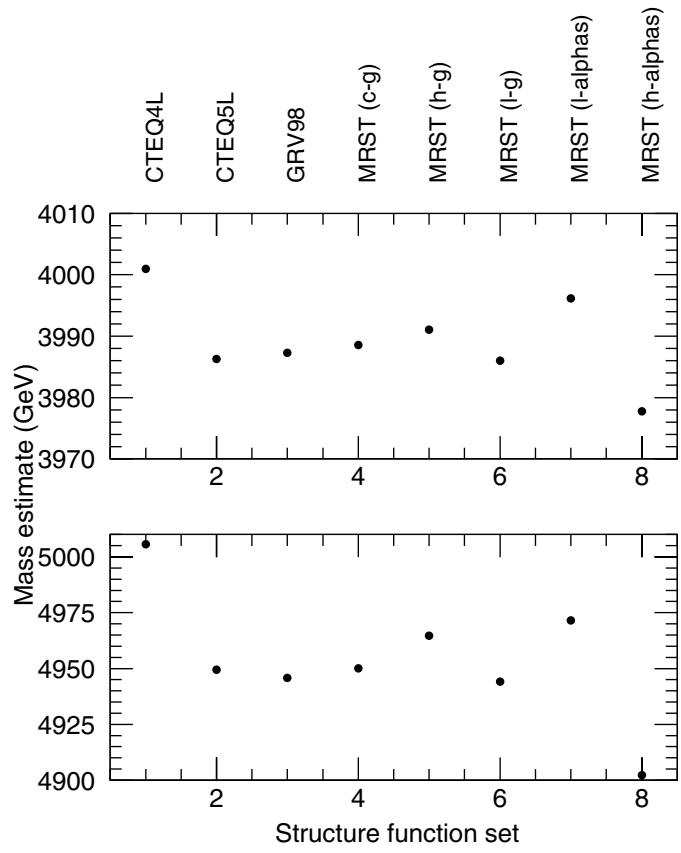

Fig. 8. M_c reconstructed values as a function of the structure function set used for the likelihood fit. The events were generated using CTEQ4L. The input values for M_c were 4 TeV (*upper plot*) and 5 TeV (*lower plot*), respectively

the effect of the ~ 20 minimum bias events superimposed to each hard interaction when running at high luminosity. The modeling of the detector response to the recoil energy was performed in UA2 and at the Tevatron using the hadronic system recoiling against the Z. A similar approach can be used for the $W^{(1)}$, for which ~ 300 $Z^{(1)}$ are available [8]. The statistical power of the sample is of course quite weak, but the relative impact of the ensuing uncertainty is expected to be much lower than for the W. In fact, the average transverse momentum of the $W^{(1)}$ is ~ 90 GeV. This should be compared *e.g.* to an average p_T^W of 6.4 GeV for UA2, yielding an uncertainty of 115 MeV on the m_T fit, dominated by the Z statistics, very similar to the $Z^{(1)}$ statistics expected for ATLAS [19], [20]. Even assuming a linear scaling with the p_T of the recoil system, the resulting uncertainty is well below 10 GeV, which is the upper limit for a single systematic contribution to be essentially negligible.

Similar considerations can be applied to the theoretical uncertainty on the shape of the transverse momentum distribution of the $W^{(1)}$, expected to bring a contribution well below 10 GeV. In order to derive a very pessimistic upper limit to this term, we generated a sample of $W^{(1)}$ events switching off the PYTHIA initial-state radiation mechanism. The average p_T was about 1.3 GeV, compared to the ~ 90 GeV of the default prescription. On these events we have then performed a likelihood fit with the theoretical histograms produced with the default PYTHIA settings. The distribution of the estimated $1/M_c^2$ is shown in Fig. 7 for a standard data set (full histogram), and for the set of experiments generated with no initial state radiation (dashed histogram). The effect is well below the statistical width of the distribution, and the central M_c value is displaced from 4002 to 4005 GeV.

The higher-order electroweak corrections, and in particular the radiative decays of the W and the $W^{(1)}$, will have a sizable effect on the shape of the transverse mass distribution. A NLO calculation and a detailed experimental study of the reconstruction of leptons in the relevant energy range will be needed.

The kinematic distribution of the lepton-neutrino system presents a shape that depends on the quark and antiquark PDF's. All the Monte Carlo samples used as data for the analysis were generated with the CTEQ4L PDF's [22]. In order to approximately study the effects of the uncertainty on the PDF parametrization, the expected transverse mass spectra, for different values of M_c, were produced with eight different structure function sets, all providing a leading order parametrization and based on recent experimental data [23] [24] [25]. The use of PDF's from different groups takes into account the uncertainties due to the the parametrisation method, and the use of five different sets from [25] gives a rough estimate of the dependence of the result on the physics assumptions entering the parametrisation procedure. As recently pointed out [26], an additional uncertainty source exists, inherent to each parametrisation, due to the experimental errors of the data used for the PDF fit. No experimental data exist at present for the kinematic region addressed by the present analysis, therefore the present PDF parametrisations, being based on extrapolations, suffer from large

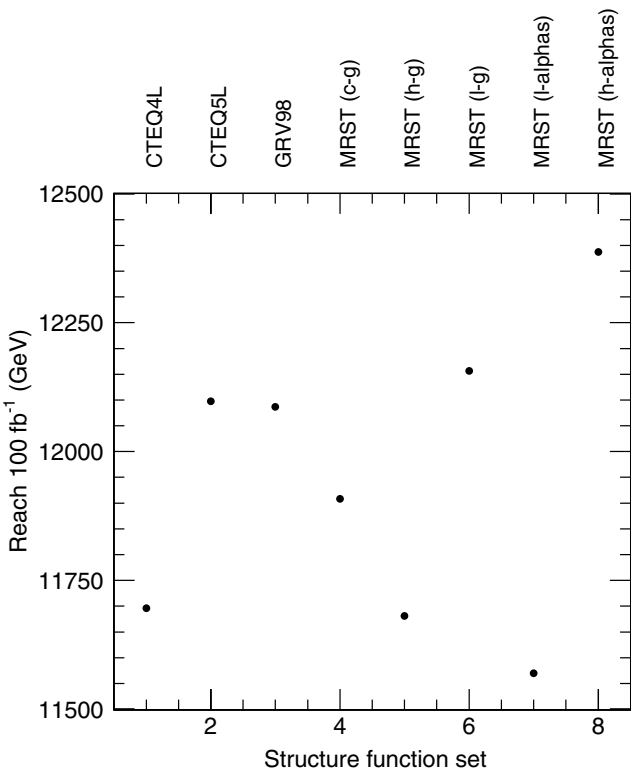

Fig. 9. Expected sensitivity (100 fb^{-1}) in GeV as a function of the structure function set used for the for the likelihood fit. The events were generated using CTEQ4L

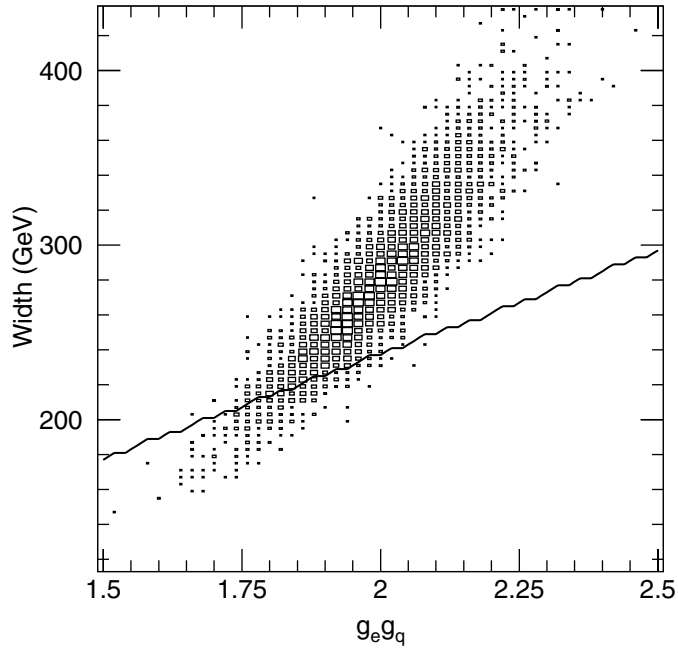

Fig. 10. Distribution of the values (P, Γ) minimizing the χ^2 for a set of $\sim$ 40000 Monte Carlo experiments. The (P, Γ) in the region below the *black line* are not compatible with the reference ADD model

uncertainties. However, when the LHC data will become available, the study of e.g. jet production at high P_T will be used to provide tight constraints on the quark PDF's in the relevant region in x and Q^2.

The reconstructed values, as a function of the PDF set, are shown in Fig. 8 for both $M_c = 4$ and 5 TeV. The spread goes from 25 GeV to 100 GeV, at 4 and 5 TeV, respectively, and it is of the same order of the r.m.s of the distributions summarized in Table 3.

The experimental sensitivity as a function of the structure function set, is shown in Fig. 9. In the worst case the difference with respect to CTEQ4L is $\sim$ 0.6 TeV. If we consider the spread of the values, we can estimate a contribution to the systematic uncertainty of $\sim$ 0.4 TeV, bringing down the sensitivity of ATLAS to this process for one year at high luminosity and one lepton flavour to $\sim$ 11.3 TeV.

5 Measurement of the coupling of $W^{(1)}$ to the fermions

Up to now we have assumed the extra dimensions model as given, and we have evaluated the statistical sensitivity of the ATLAS experiment as a function of the single parameter M_c which determines the model.

The next step is to study the precision with which the ATLAS detector can measure the couplings of the $W^{(1)}$ to fermions. We still assume the full tower structure of the ADD model, and the fact that the $W^{(n)}$ couple only to left-handed fermions as its Standard Model counterpart. In this situation, only two couplings enter the cross section formula, g^e and g^q, which are the same for all values of n, and are equal to $\sqrt{2}$ times the SM couplings (Sect. 1).

The shape of the invariant transverse mass is sensitive to the product of the two couplings ($P = g^e \times g^q$) through the normalization with respect to the SM W production, and to the width of the $W^{(1)}$ (Γ), which for our model is related to the couplings by (4).

The fit should be performed (and it will indeed be performed in a real experiment) at the same time on the three variables M_c, P and Γ. We are interested here on evaluating if the m_T distribution displays any sensitivity to the coupling of the fermions to the $W^{(1)}$, therefore we unrealistically assume M_c fixed at the nominal value of 4 TeV, and we perform the likelihood minimization only on P and Γ.

We generated the invariant transverse mass distribution for P varying in the range $1.5 \rightarrow 2.5$ in steps of 0.025 and Γ in the range $115 \rightarrow 435$ GeV in steps of 2 GeV.

The "data" are a set of events generated for the nominal value $P = 2$ and $\Gamma(W^{(1)}) = 277$ GeV, out of which we produce a set of Monte Carlo experiments, each corresponding to a statistics of 100 fb^{-1}.

For each experiment, the binned likelihood was calculated according to (7) on the transverse mass interval $1 \rightarrow$ 10 TeV, and the (P,Γ) pair maximizing the likelihood was estimated. The distribution of the χ^2 minima in the (P,Γ) plane is shown Fig. 10 for a set of $\sim$40000 Monte Carlo experiments. The distribution is centered around the input values, and the two variables are correlated, re-

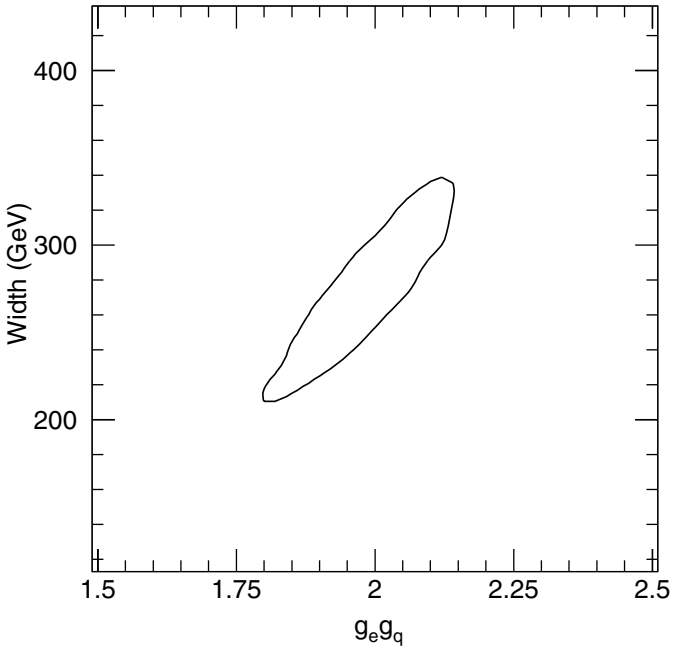

Fig. 11. Ellipsoid in the (P,Γ) plane limiting the 68% CL region for the simultaneous measurement of the two parameters

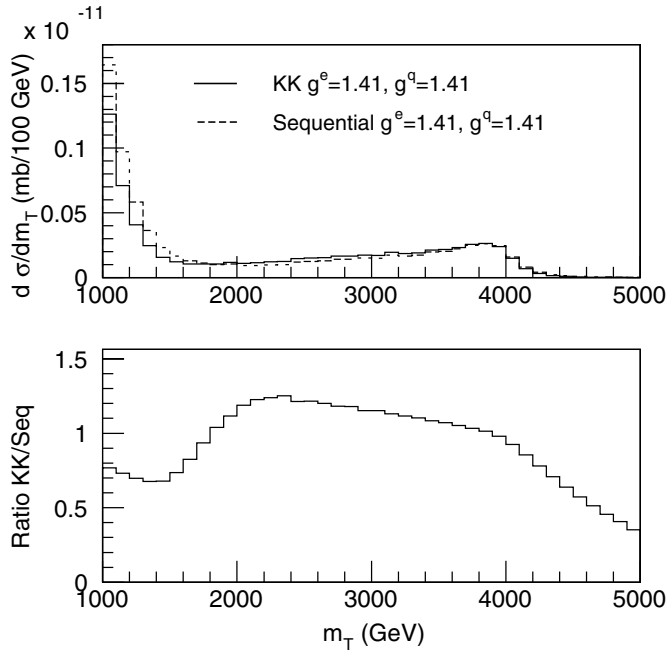

Fig. 13. a Invariant transverse mass for the reference KK model (*full line*) and for the sequential model (*dashed line*). **b** Ratio between the two distribution as a function of the transverse mass

flecting the fact that a small loss in absolute cross section can be compensated by a narrower peak distribution.

The ellipsoid in the (P,Γ) plane limiting the 68% CL region for the simultaneous measurement of the two variables is shown in Fig. 11. The limiting values are respectively $1.8 < P < 2.15$, and $210 < \Gamma < 340$ GeV.

If we specialize to our reference model, and we assume for Γ the dependence from the couplings given by (4), we can extract from the (P,Γ) measurement a measurement of the couplings by solving a system of the form:

$$\begin{cases} P = g^e(n)\, g^q(n) \\ \Gamma \propto a\, g^e(n)^2 + b\, g^q(n)^2 \end{cases}$$

In the region of the (P,Γ) plane above the black line in Fig. 10 this system has two solutions, whereas below the line the system has no solution. Approximately 8% of the experiments fall in the region incompatible with the input model. For these no measurement of the couplings is possible. It is however still possible to verify the compatibility with the input model by considering the error on the measured (P,Γ) pair extracted from the likelihood shape.

The distribution of the two solutions of the system in the (g^e, g^q) plane is shown in Fig. 12. If we calculate the region including 68% of the experiments for the solution with lower g^e, the resulting ellipsoid is limited by the values: $1.25 < g^e < 1.55$ and $1.2 < g^q < 1.7$.

The results shown here are valid for $M_c = 4$ TeV. We have performed the same study for $M_c = 5$ TeV, and in this case $\sim 30\%$ of the experiments yield a (P,Γ) measurement compatible with the input model, indicating that the sensitivity to the $W^{(1)}$ width is progressively lost with increasing M_c. Starting from value of 6 TeV, the only observable effect is in the interference region, which can be parametrized as $g^e g^q / M_c^2$. Therefore in this case only the product of the two couplings can be measured.

6 Discrimination of models

Additional heavy gauge bosons arise in many extensions of the Standard Model, as the result of a richer gauge structure of the theory. Typical examples are grand unified theories, superstring theories, the left-right symmetric model [27], and, more recently, the "little Higgs" model [28].

The essential feature distinguishing the reference KK model is the presence of the tower of equally spaced KK resonances. As remarked above, even for the lowest considered M_c value of 4 TeV, the second resonance is not accessible to LHC experiments. The presence of the additional resonances does however distort the shape of transverse mass distribution at values much lower than the mass of the second resonance.

In order to evaluate if this effect is statistically observable with 100 fb^{-1} of integrated luminosity, we compare the reference model to a toy "sequential" model, where a single left-handed W' is produced, corresponding to the matrix element of (3), where the sum on the second term contains the single term $n = 1$. We take for this model couplings to fermions equal to those of the Standard Model ones multiplied by $\sqrt{2}$. In the region of interference with the SM W, corresponding to an interval in $\hat{s}$ between 1 and 2 TeV, the loss of cross section with respect to the SM is $\sim$ a factor 2 for the KK model, and a factor $\pi^2/6$ smaller for the "sequential" model. This is reflected in the distribution of the transverse mass, as can be seen in the

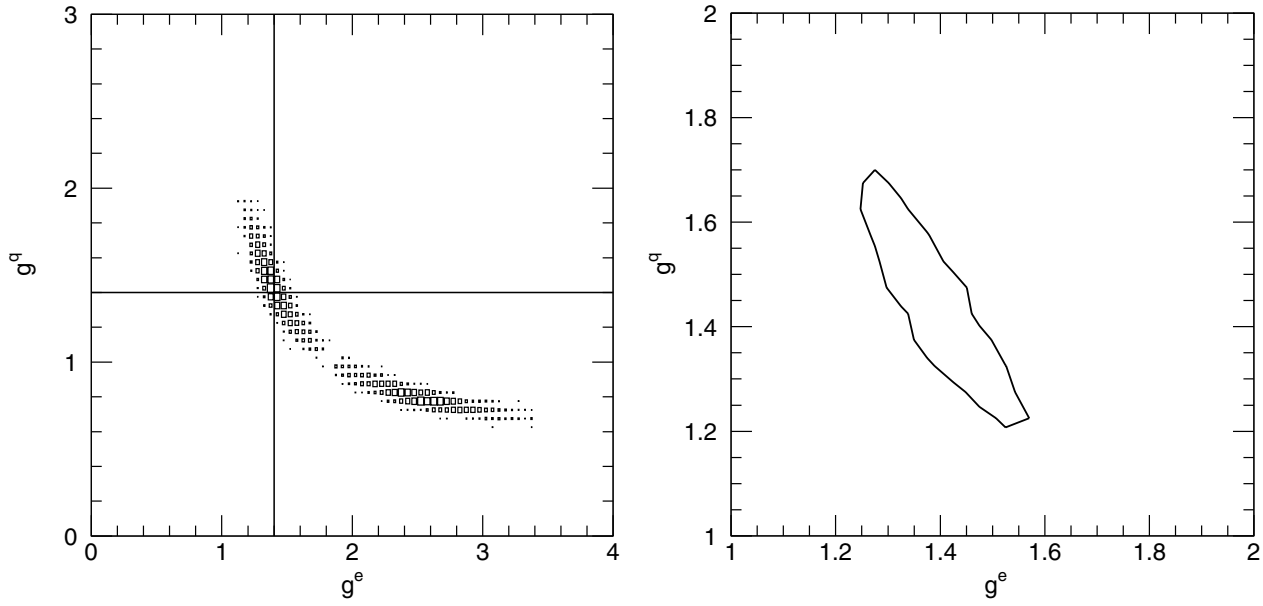

Fig. 12. *Left:* Distribution of the values (g^e, g^q) minimizing the χ^2 for a set of ~ 4000 Monte Carlo experiments. *Right:* Ellipsoid in the (g^e, g^q) plane limiting the 68% CL region for the simultaneous measurement of the two parameters

upper part of Fig. 13, where the shapes for the reference model (full line) and the sequential model (dashed line) are compared.

The relevant question at this point is if a combination of M_c, g^e, and g^q exists such that the predictions of a sequential model could give a good fit to a set of events generated with the reference KK model. Only the couplings need to be varied, as the mass of the W' is approximately fixed by the position of the edge.

A set of theoretical histograms for the sequential model with $M_c = 4$ TeV, was generated by varying the values of g^e and g^q.

We use as "data" the same set of events generated for the reference KK model with $M_c = 4$ TeV, and the default model values $g^e(n) = g^q(n) = \sqrt{2}$.

The χ^2 values obtained in the previous section can thus be compared with the χ^2 values obtained in the minimization performed according to the sequential model. The two χ^2 distributions are shown in Fig. 14. The fit is performed on a transverse mass interval $1 \rightarrow 5$ TeV, corresponding to 40 bins, and since the highest few bins typically contain less than 5 events, the two distributions are only an approximation to real χ^2 distributions. It is however clear from the closeness of the two that the ATLAS experiment, with an integrated luminosity of 100 fb^{-1}, has little discrimination power between the two models (Fig. 15), which were deliberately chosen to be identical in all except in the presence of the KK tower of excitations.

This result is in agreement with a similar exercise performed for the $Z^{(1)}$ in [9]. An extension of the analysis to take into account the full kinematic information, including angular and rapidity distributions would not yield a significant improvement in discrimination power. As remarked in [9], in the reference model for this study the leptons and the quarks are at the same orbifold point,

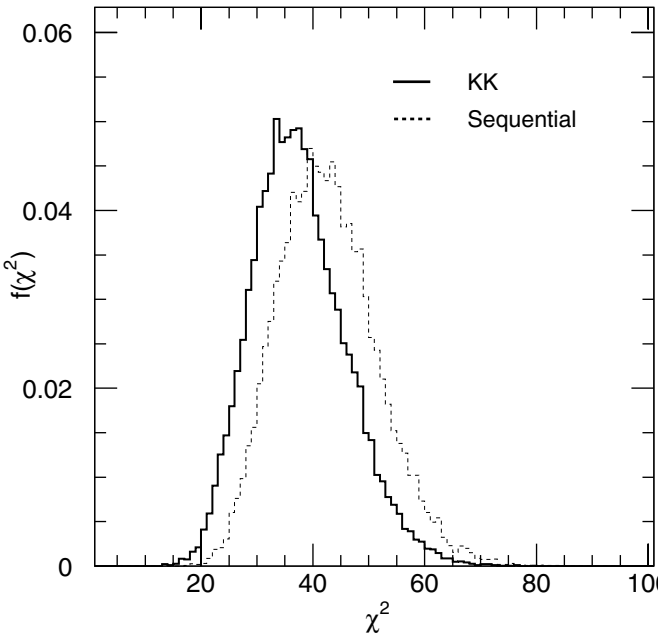

Fig. 14. Minimum χ^2 for the KK model (*full line*) and for the sequential model (*dashed line*). This fit was performed on the transverse mass interval $1 \rightarrow 5$ TeV

thus yielding an interference pattern very similar to the one of a sequential boson. A KK model where the leptons and the quarks are at opposite fixed point of the orbifold would yield a positive interference with the SM W easily distinguishable from the sequential toy model.

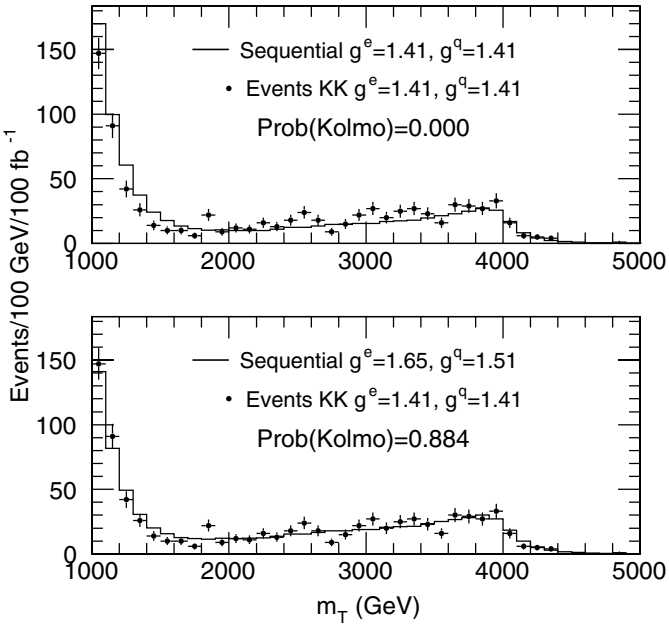

Fig. 15. Comparisons of the predictions for the sequential model (*full line*) with one 100 fb^{-1} experiment generated with the reference KK model. The assumed values of the couplings for the sequential model are ($\sqrt{2}$, $\sqrt{2}$) (*upper plot*) and (1.65, 1.51) (*lower plot*). With an appropriate choice of the coupling constants, the prediction can be made to describe the data

7 Conclusions

A detailed study of the leptonic signatures for the production of the KK excitations of the W boson in models with TeV-scale extra dimensions has been performed.

The production and decay of the excitations were fully simulated, including initial state QCD radiation, and the resulting particles were passed through a parametrized simulation of the ATLAS detector.

We found that with an integrated luminosity of 100 fb^{-1} ATLAS will be able to detect a peak in the lepton-neutrino invariant transverse mass if the compactification scale is below 6.0 TeV.

Even in absence of a peak, a detailed study of the transverse mass shape will allow to observe a deviation from the Standard Model due to the interference of the KK excitations with the SM bosons. From a study based on a maximum likelihood estimation of the compactification mass, ATLAS will be able to exclude at 95% CL a signal from the model considered in this work for $M_c < 11.7$ TeV, for one lepton flavour and with an integrated luminosity of 100 fb^{-1}, neglecting systematic effects.

We have performed an evaluation of the influence of experimental and theoretical uncertainties on this result. The resulting uncertainties due to the lepton energy and momentum scale, the energy and momentum resolution, the p_T^ν measurement and the knowledge of the $W^{(1)}$ p_T spectrum should be below 10 GeV (whereas the statistical error on the compactification mass measurement goes from $\sim 0.5\%$ at 4 TeV, to $\sim 2\%$ at 6 TeV).

The maximum effect observed from the consideration of various set of PDF's is a reduction of order ~ 0.4 TeV on the achievable limit, bringing down the sensitivity to ~ 11.3 TeV.

We have also studied the properties of the observed resonance. In particular, the precision with which the ATLAS detector can measure the couplings of the $W^{(1)}$ to the fermions has been established. For the lowest allowed $W^{(1)}$ masses the precision of 10 to 20% of the W coupling to fermions can be achieved for $M_c = 4$ TeV, but the sensitivity is quickly lost with increasing M_c.

Another important question is the assessment of the model which has produced the signal detected. The essential feature characterizing the model considered in this work is the presence of equally spaced KK resonances. From the comparison with a model with a single W' produced, we see that from the consideration of the transverse mass spectra alone, the presence of the tower of KK resonances cannot be detected at LHC.

Acknowledgements. This work has been performed within the ATLAS collaboration, and we thank collaboration members for helpful discussions. We have made use of the physics analysis and simulation tools which are the result of collaboration-wide efforts. We gratefully acknowledge enlightening discussions with Georges Azuelos, Roberto Ferrari and Giorgio Goggi.

References

1. N. Arkani-Hamed, S. Dimopoulos, G. Dvali: Phys. Lett. B **249**, 263 (1998)
   Phys. Rev. D **59**, 086004 (1999)
2. For a summary of the very extensive literature on the subject, see: J.A. Hewett and M. Spiropulu: *Particle Physics Probes Of Extra Spacetime Dimensions.* hep-ph/0205106, and references therein
3. K. Dienes, E. Dudas, and T. Gherghetta: Nucl. Phys. B **537**, 47 (1999)
4. A. Pomarol, M. Quirós: Phys. Lett. B **438**, 255 (1998)
   M. Masip, A. Pomarol: Phys. Rev. D **60**, 096005 (1999)
   I. Antoniadis, K. Benakli, M. Quirós: Phys. Lett. B **460**, 176 (1999)
5. T.G. Rizzo: Phys.Rev. D **61**, 055005 (2000)
6. P. Nath and M. Yamaguchi: Phys. Rev. D **60** (1999) 116004
   P. Nath, Y. Yamada, M. Yamaguchi: Phys. Lett. B **466**, 100 (1999)
7. F. Cornet, M. Relaño, and J. Rico: Phys. Rev. D **61**, 037701 (2000)
8. G. Azuelos and G. Polesello: in proceedings of the Workshop 'Physics at TeV Colliders', Les Houches, France, 21 May – 1 June 2001, hep-ph/0204031 (2002); G. Azuelos and G. Polesello: *Prospects for the observations of Kaluza-Klein excitations of gauge bosons in the ATLAS detector* ATLAS Scientific Note SN-ATLAS-2003-023, to be published in EPJ Direct, Sect. A–E
9. T. Rizzo: *Distinguishing Kaluza-Klein Resonances From a Z′ in Drell-Yan Processes at the LHC* hep-ph/0109179
10. C.D. McMullen, S. Nandi: hep-ph/0110275
11. T. Sjöstrand: Comp. Phys. Comm. series **82**, 74 (1994)

12. E. Richter-Was, D. Froidevaux, L. Poggioli: *ATLFAST 2.0: a fast simulation package for ATLAS* ATLAS Internal Note ATL-PHYS-98-131 (1998)
13. N. Arkhani-Hamed, M. Schmaltz: Phys. Rev. D **61**, 033005 (2000)
14. S. Baker, R. Cousins: Nucl. Instrum. Methods **221**, 437 (1984)
15. G.J. Feldman, R.D. Cousins: Phys. Rev. D **57**, 3873 (1998)
16. D.E. Groom et al.: Particle Data Group: *Review of Particle Physics*, Eur Phys. J. C. **15** (2000)
17. ATLAS Collaboration: "*ATLAS Technical Design Report*", CERN/LHCC/99-14/15 (1999)
18. G. Altarelli, M. L. Mangano: "*Electroweak Physics*", in the Proceedings of the 1999 CERN Workshop on Standard Model Physics (and more) at the LHC, CERN, Geneve, Switzerland, CERN-2000-004
19. J. Alitti et al. (UA2 collaboration): Phys. Lett. B **241**, 150 (1990)
20. J. Alitti *et al.* (UA2 collaboration): Z. Phys. C **47**, 523 (1990)
21. U. Baur, O. Brein, W. Hollik, C. Schappacher, D. Wackeroth: Phys. Rev. D **65**, 033007 (2002)
22. H.L. Lai, J. Huston, S. Kuhlmann, F. Olness, J. Owens, D. Soper, W.K. Tung, H. Weerts: Phys. Rev. D **55**, 1280 (1997)
23. H.L. Lai, J. Huston, S. Kuhlmann, J. Morfin, F. Olness, J. Owens, J. Pumplin, W.K. Tung: Eur. Phys. J. C **12**, 375 (2000)
24. M. Glück, E. Reya, A. Vogt: Eur. Phys. J. C **5**, 461 (1998)
25. A.D. Martin, R.G. Roberts, W. J. Stirling, R. S. Thorne: Eur. Phys. J. C **4**, 463 (1998)
26. S. Alekhin et al.: *The QCD/SM Working Group. Summary Report*, proceedings of the Workshop: "Physics at TeV Colliders", Les Houches, France, 21 May – 1 June 2001, hep-ph/0204316
27. For a summary of models featuring extra W bosons see: M. Cvetic, S. Godfrey: "Discovery and identification of extra gauge bosons" in *Eletroweak Symmetry Breaking and Beyond the Standard Model*, T. Barklow, S. Dawson, H. Haber, and J. Siegrist, eds. (World Scientific 1995) hep-ph/9504216
28. T. Han, H.E Logan, B. McElrath, L.T. Wang: Phys.Rev. D **67**, 095004 (2003), and references therein